

# A test for a conjunction\*

K.J. Worsley<sup>a,†</sup>, K.J. Friston<sup>b</sup>

<sup>a</sup>*Department of Mathematics and Statistics, McGill University, Montreal, Canada H3A 2K6*

<sup>b</sup>*Wellcome Department of Cognitive Neurology, Institute of Neurology, Queen Square, London WC1N 3BG, UK*

---

## Abstract

A conjunction is defined in the brain mapping literature as the occurrence of the same event at the same location in two or more independent 3D brain images. The images are smooth isotropic 3D random fields of test statistics, and the event occurs when the image exceeds a fixed high threshold. We give a simple approximation to the probability of a conjunction occurring anywhere in a fixed region, so that we can test for a local increase in mean of the images at the same unknown location in all images, a generalization of the split- $t$  test. This is the corollary to a more general result on the expected Minkowski functionals of the set of points where a conjunction occurs.

*MSC:* 60G60, 62M09

*Keywords:* Split- $t$  test; random field; Euler characteristic; integral geometry; stereology.

---

## 1 Introduction

Let  $X_i(\mathbf{t})$  be the value of image  $i$  at location  $\mathbf{t} \in \mathfrak{R}^D$ ,  $1 \leq i \leq n$ , and let  $x$  be a fixed threshold. The set of points where a conjunction occurs is

$$C = \{\mathbf{t} \in S : X_i(\mathbf{t}) \geq x \text{ for all } 1 \leq i \leq n\}.$$

An example is shown in Figure 1 for  $n = 6$ . We are interested in the probability that  $C$  is not empty, that is, the probability that all images exceed the threshold at some point inside  $S$ , or that the maximum over  $\mathbf{t} \in S$  of the minimum over  $i$  of  $X_i(\mathbf{t})$  exceeds  $x$ :

$$\mathcal{P}\{C \neq \emptyset\} = \mathcal{P}\left\{\max_{\mathbf{t} \in S} \min_{1 \leq i \leq n} X_i(\mathbf{t}) \geq x\right\}. \quad (1)$$

---

\*Research supported by the Natural Sciences and Engineering Research Council of Canada, Fonds pour la Formation des Chercheurs et l'Aide à la Recherche de Québec, and the Wellcome Trust

†Corresponding author. Tel.: +1-514-398-3842; fax: -3899; e-mail: [worsley@math.mcgill.ca](mailto:worsley@math.mcgill.ca); web: <http://www.math.mcgill.ca/~keith>.

If the images are independent stationary random fields then the expected Lebesgue measure or volume of  $C$  is

$$\mathcal{E}\{|C|\} = p^n |S|, \quad (2)$$

where  $p = \mathcal{P}\{X_i(\mathbf{t}) \geq x\}$ . Our main result is that (2) holds if Lebesgue measure is replaced by a vector of Minkowski functionals, and  $p$  is replaced by a matrix of Euler characteristic intensity functions for the random field. This gives (2) as a special case, and other interesting quantities such as the expected surface area of  $C$ , which comes from the  $D - 1$  dimensional Minkowski functional. But the component of most interest to us is the zero dimensional Minkowski functional, or Euler characteristic (EC). For high thresholds, the expected EC of  $C$  is a very accurate approximation to the probability (1) that we seek (Adler, 1998). We apply this result to some real data in brain mapping in Section 5.

This also allows us to set the level of the split- $t$  test. Shaywitz *et al.* (1995) used this test to determine whether the functional organization of the brain for language differed according to sex. 38 independent fMRI images were randomly divided into  $n = 2$  groups, and an image  $X_i(\mathbf{t})$  of  $t$ -statistics was calculated for each group  $i = 1, 2$ . The split- $t$  test rejects if the null hypothesis is rejected for both groups at the same point  $\mathbf{t}$ , that is, if  $X_1(\mathbf{t}) \geq x$  and  $X_2(\mathbf{t}) \geq x$  for some threshold  $x$ , taken as the upper level 5% point of the  $t$ -distribution with 17 degrees of freedom. The resulting image of conjunctions  $C$  appears on the cover of *Nature* that contains Shaywitz *et al.* (1995).

## 2 Integral geometry and stereology

In this section we shall state some results from integral geometry and stereology that will be used to prove our main result (see for example Santaló, 1976).

Let  $\mu_i(A)$  be the  $i$ th Minkowski functional of a set  $A \subset \mathfrak{R}^D$ , scaled so that it is invariant under embedding of  $A$  into any higher dimensional Euclidean space. If  $A$  has a twice differentiable boundary  $\partial A$ , then it can be defined as follows. Let  $s_i = 2\pi^{i/2}/\Gamma(i/2)$  be the surface area of a unit  $(i - 1)$ -sphere in  $\mathfrak{R}^i$ . For  $\mathbf{M}$  an  $m \times m$  matrix let  $\text{detr}_j(\mathbf{M})$  denote the sum of the determinant of all  $j \times j$  principal minors of  $\mathbf{M}$ , so that  $\text{detr}_m(\mathbf{M}) = \det(\mathbf{M})$ ,  $\text{detr}_1(\mathbf{M}) = \text{tr}(\mathbf{M})$  and we define  $\text{detr}_0(\mathbf{M}) = 1$ . Let  $\mathbf{Q}$  be the  $(D - 1) \times (D - 1)$  curvature matrix of  $\partial A$ . Then for  $0 \leq i < D$

$$\mu_i(S) = \frac{1}{s_{D-i}} \int_{\partial A} \text{detr}_{D-1-i}(\mathbf{Q}) dt,$$

and define  $\mu_D(A) = |A|$ . Note that  $\mu_0(A)$  is the EC of  $A$  by the Gauss-Bonnet Theorem, and  $\mu_{D-1}(A)$  is half the surface area of  $A$ . For example, the Minkowski functionals of a ball of radius  $r$  in  $\mathfrak{R}^3$  are

$$\mu_0(S) = 1, \quad \mu_1(S) = 4\pi r, \quad \mu_2(S) = 2\pi r^2, \quad \mu_3(S) = (4/3)\pi r^3. \quad (3)$$

We shall use the result that any set functional  $\psi(A)$  that obeys the additivity rule

$$\psi(A \cup B) = \psi(A) + \psi(B) - \psi(A \cap B) \quad (4)$$

is a linear combination of the Minkowski functionals. Let  $A, B \subset \mathfrak{R}^D$ , then the Kinematic Fundamental Formula of integral geometry relates the integrated EC of the intersection of  $A$  and  $B$  to their Minkowski functionals:

$$\int \mu_0(A \cap B) = s_2 \dots s_D \sum_{i=0}^D \frac{\mu_i(A) \mu_{D-i}(B)}{c_i^D}, \quad (5)$$

where the integral is over all rotations and translations of  $A$ , keeping  $B$  fixed, and

$$c_i^D = \frac{\Gamma\left(\frac{1}{2}\right) \Gamma\left(\frac{D+1}{2}\right)}{\Gamma\left(\frac{i+1}{2}\right) \Gamma\left(\frac{D-i+1}{2}\right)}.$$

### 3 Random fields

If  $X(\mathbf{t})$ ,  $\mathbf{t} \in \mathfrak{R}^D$ , is an isotropic random field with excursion set  $A = \{\mathbf{t} : X(\mathbf{t}) \geq x\}$  then

$$\mathcal{E}\{\mu_0(A \cap S)\} = \sum_{i=0}^D \rho_i \mu_i(S) \quad (6)$$

for some constants  $\rho_i$ . This follows from the fact that  $\psi(S) = \mathcal{E}\{\mu_0(S \cap A)\}$  obeys the additivity rule (4), since  $\mu_0$  does, so it must be a linear combination of the Minkowski functionals  $\mu_i(S)$ . The coefficients  $\rho_i$ , called Euler characteristic (EC) intensities in  $\mathfrak{R}^i$ , can be evaluated for a variety of random fields (Adler, 1981; Worsley, 1994, 1998; Siegmund & Worsley, 1995; Cao & Worsley, 1999ab). For example, for a Gaussian random field with  $\mathcal{E}\{X(\mathbf{t})\} = 0$ ,  $\mathcal{V}ar\{X(\mathbf{t})\} = 0$ ,  $\mathcal{V}ar\{\partial X(\mathbf{t})/\partial \mathbf{t}\} = \lambda \mathbf{I}$ , where  $\mathbf{I}$  is the  $D \times D$  identity matrix, then  $\rho_0 = \mathcal{P}\{X(\mathbf{t}) \geq x\}$  and for  $i > 0$

$$\rho_i = \lambda^{i/2} (2\pi)^{-(i+1)/2} \text{He}_{i-1}(x) e^{-x^2/2}, \quad (7)$$

where  $\text{He}_j(x)$  is the Hermite polynomial of degree  $j$  in  $x$ . We now extend (6) to higher Minkowski functionals.

#### Lemma 1

$$\mathcal{E}\{\mu_i(A \cap S)\} = \sum_{j=i}^D c_i^j \rho_{j-i} \mu_j(S).$$

**Proof.** Clearly  $\psi(S) = \mathcal{E}\{\mu_i(A \cap S)\}$  obeys the additivity rule (4), since  $\mu_i$  does, so that we can write

$$\mathcal{E}\{\mu_i(A \cap S)\} = \sum_{j=0}^D a_{ij} \mu_j(S) \quad (8)$$

for some constants  $a_{ij}$  that do not depend on  $S$ . To evaluate these constants, replace  $S$  in (8) by  $E_k$ , a bounded convex set in a  $k$ -plane,  $k \leq D$ . Since the  $i$ th Minkowski functional of a set in  $\mathfrak{R}^k$  is zero for  $i > k$ , then  $a_{ik}$  is zero for  $i > k$ . For  $i \leq k$ ,

$$\frac{\mathcal{E}\{\mu_i(A \cap E_k)\}}{\mu_k(E_k)} = \sum_{j=i}^D a_{ij} \frac{\mu_j(E_k)}{\mu_k(E_k)} \rightarrow a_{ik} \quad (9)$$

as  $E_k \rightarrow \mathfrak{R}^k$ . We can thus interpret  $a_{ik}$  as the density of the  $i$ th Minkowski functional of the excursion set of  $X$  in  $\mathfrak{R}^k$ . To evaluate  $a_{ik}$ , apply the Kinematic Fundamental Formula (5) to  $A \cap E_D$  and  $S$ :

$$\int \mu_0((A \cap E_D) \cap S) = s_2 \dots s_D \sum_{i=0}^D \frac{\mu_i(A \cap E_D) \mu_{D-i}(S)}{c_i^D}.$$

Dividing both sides by  $s_2 \dots s_D \mu_D(E_D)$  and taking limits we get

$$\mathcal{E}\{\mu_0(A \cap S)\} = \sum_{i=0}^D \lim_{E_D \rightarrow \mathfrak{R}^D} \frac{\mathcal{E}\{\mu_i(A \cap E_D)\} \mu_{D-i}(S)}{\mu_D(E_D) c_i^D}.$$

Comparing this with (6) we get

$$\lim_{E_D \rightarrow \mathfrak{R}^D} \frac{\mathcal{E}\{\mu_i(A \cap E_D)\}}{\mu_D(E_D)} = c_i^D \rho_{D-i}$$

and combining this with (9), we get for  $i \leq j$ ,

$$a_{ij} = c_i^j \rho_{j-i}.$$

Substituting into (8) completes the proof.  $\square$

## 4 Geometry of the set of conjunctions

**Theorem 2** Let  $b_i = \Gamma((i+1)/2)/\Gamma(1/2)$  and define the upper triangular Toeplitz matrix  $\mathbf{R}_k$  and the vector  $\mu(B)$  by

$$\mathbf{R}_k = \begin{pmatrix} \rho_{0k}/b_0 & \rho_{1k}/b_1 & \cdots & \rho_{Dk}/b_D \\ 0 & \rho_{0k}/b_0 & \cdots & \rho_{(D-1)k}/b_{D-1} \\ \vdots & & \ddots & \vdots \\ 0 & 0 & \cdots & \rho_{0k}/b_0 \end{pmatrix}, \quad \mu(B) = \begin{pmatrix} \mu_0(B)b_0 \\ \mu_1(B)b_1 \\ \vdots \\ \mu_D(B)b_D \end{pmatrix},$$

where  $\rho_{ik}$  is the EC intensity of  $X_k(\mathbf{t})$  in  $\mathfrak{R}^i$ ,  $1 \leq k \leq n$ , and  $B \subset \mathfrak{R}^D$ . Then

$$\mathcal{E}\{\mu(C)\} = \left( \prod_{i=1}^n \mathbf{R}_i \right) \mu(S).$$

**Proof.** The proof follows by induction on  $n$ . From the lemma, we see that it is clearly true for  $n = 1$ . Let  $A_k$  be the excursion set for  $X_k(\mathbf{t})$ , so that  $C = A_1 \cap \dots \cap A_n \cap S$ . If the result is true for  $n = k$  then by first conditioning on  $A_{k+1}$  and replacing  $S$  by  $A_{k+1} \cap S$  we get

$$\mathcal{E}\{\mu(A_1 \cap \dots \cap A_k \cap (A_{k+1} \cap S))\} = \left( \prod_{i=1}^k \mathbf{R}_i \right) \mathcal{E}\{\mu(A_{k+1} \cap S)\} = \left( \prod_{i=1}^k \mathbf{R}_i \right) \mathbf{R}_{k+1} \mu(S)$$

by the result for  $n = 1$ . This completes the proof.  $\square$

Comparing this result with (2) we see that it has the same form, with volume replaced by the vector of weighted Minkowski functionals, and probability replaced by the matrix of weighted EC intensities. The last element is the same as (2), and the first element is the expected EC of the set of conjunctions that we shall use as an approximation to the probability of a conjunction anywhere in  $S$ :

$$\mathcal{P}\{C \neq \emptyset\} = \mathcal{P}\left\{\max_{\mathbf{t} \in S} \min_{1 \leq i \leq n} X_i(\mathbf{t}) \geq x\right\} \approx (1, 0, \dots, 0) \left(\prod_{i=1}^n \mathbf{R}_i\right) \mu(S), \quad (10)$$

for high thresholds  $x$ .

## 5 Application

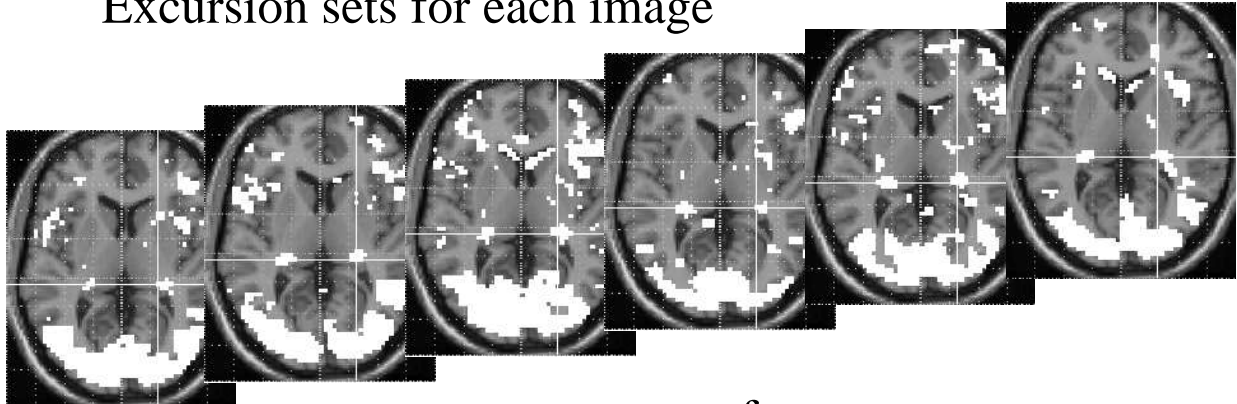
We shall apply the result to some  $D = 3$  dimensional functional magnetic resonance imaging (fMRI) data fully described in Friston *et al.* (1999). The purpose of the experiment was to determine those regions of the brain that were consistently stimulated by all subjects while viewing a pattern of radially moving dots. To do this, subjects were presented with a pattern of moving dots, followed by a pattern of stationary dots, and this was repeated 10 times, during which a total of 120 3D fMRI images were obtained at the rate of one every 3.22 seconds. For each subject  $i$  and at every point  $\mathbf{t} \in \mathfrak{R}^3$ , a test statistic  $X_i(\mathbf{t})$  was calculated for comparing the fMRI response between the moving dots and the stationary dots. Under the null hypothesis of no difference,  $X_i(\mathbf{t})$  was modeled as an isotropic Gaussian random field with zero mean, unit variance and  $\lambda = 4.68\text{cm}^{-2}$ . A threshold of  $x = 1.64$ , corresponding to an uncorrected level 5% test, was chosen, and the excursion sets for each subject are shown in Figure 1, together with their intersection, which forms the set of conjunctions  $C$ . The search region  $S$  is the whole brain area that was scanned, which was an approximate spherical region with a volume of  $|S| = 1226\text{cm}^3$ . Finally, the approximate probability of a conjunction, calculated from (3), (7) and (10), is 0.0126. We can thus conclude, at the 1.26% level, that conjunctions have occurred in the visual cortex, and more interesting, the lateral geniculate nuclei (see Figure 1).

## References

- Adler, R.J., 1981. *The Geometry of Random Fields*. Wiley, New York.
- Adler, R.J., 1998. On excursion sets, tube formulae, and maxima of random fields. *Annals of Applied Probability*, in press.
- Cao, J., Worsley, K.J., 1999a. The detection of local shape changes via the geometry of Hotelling's  $T^2$  fields. *Annals of Statistics*, accepted (subject to revision).
- Cao, J., Worsley, K.J., 1999b. The geometry of correlation fields with an application to functional connectivity of the brain. *Annals of Applied Probability*, in press.
- Friston, K.J., Holmes, A.P., Price, C.J., Büchel, C., Worsley, K.J., 1999. Multi-subject fMRI studies and conjunction analyses. *NeuroImage*, in press.
- Santaló, L.A., 1976. *Integral Geometry and Geometric Probability*. *Encyclopedia of Mathematics and its Applications*, Volume 1, (Editor G-C. Rota). Addison-Wesley, Reading, Massachusetts.

- Shaywitz, B.A., Shaywitz, S.E., Pugh, K.R., 1995. Sex differences in the functional organization of the brain for language. *Nature*, **373**, 607-609.
- Siegmund, D.O., Worsley, K.J., 1995. Testing for a signal with unknown location and scale in a stationary Gaussian random field. *Annals of Statistics*, **23**, 608-639.
- Worsley, K.J., 1994. Local maxima and the expected Euler characteristic of excursion sets of  $\chi^2$ ,  $F$  and  $t$  fields. *Advances in Applied Probability*, **26**, 13-42.
- Worsley, K.J., 1998. Testing for signals with unknown location and scale in a  $\chi^2$  random field, with an application to fMRI. *Advances in Applied Probability*, accepted (subject to revision).

## Excursion sets for each image



## Conjunction: intersection of excursion sets

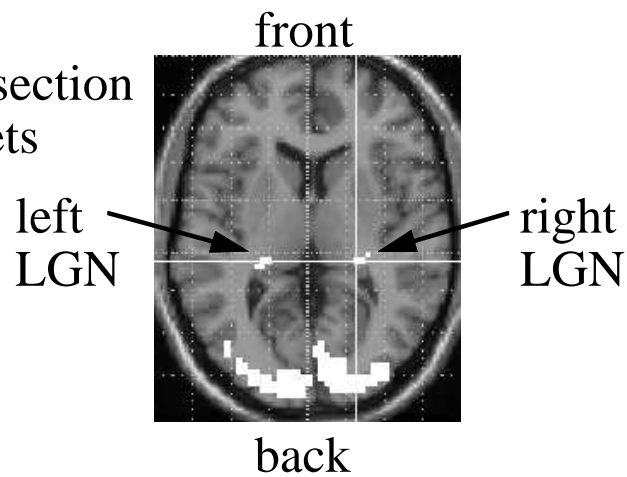


Figure 1: Conjunction of  $n = 6$  fMRI images during a visual task (only one slice of the 3D data is shown). The excursion sets of each  $X_i(\mathbf{t}) \geq 1.64$ ,  $i = 1, \dots, 6$  are shown in white on a background of brain anatomy (top). The set of conjunctions  $C$  is the intersection of these sets (bottom). The visual cortex at the back of the brain appears in  $C$ , but the most interesting feature is the appearance of the lateral geniculate nuclei (LGN) (arrows).